Structural Impact Assessment of Low Level Jets over Wind Turbines

W GUTIERREZ[1], G ARAYA[1], V P KILIYANPILAKKIL[3], A RUIZ-COLUMBIE[2], M TUTKUN[4,5], AND L CASTILLO[1]

[1] DEPARTMENT OF MECHANICAL ENGINEERING, TEXAS TECH UNIVERSITY, LUBBOCK, TX, USA

[2] NATIONAL WIND INSTITUTE, TEXAS TECH UNIVERSITY, LUBBOCK, TX, USA

[3] DEPARTMENT OF MARINE, EARTH, AND ATMOSPHERIC SCIENCES; NORTH CAROLINA STATE UNIVERSITY, RALEIGH, NC, USA

[4] INSTITUTE FOR ENERGY TECHNOLOGY (IFE), KJELLER, NORWAY

[5] UNIVERSITY OF OSLO, DEPARTMENT OF MATHEMATICS, OSLO, NORWAY

Grant: NSF-CBET #1157246, NSF-OISE-1243482 and NSF-CMMI #1100948

Presentation
for NAWEA Symposium 2015,
Blacksburg, VA.

Motivation

Understand the dynamic of the Low Level Jet (LLJ) in relation to wind turbines performance.

Objectives

- Determine the dimensions and main features of the LLJ.
- How they impact on turbines in terms of energy production and mechanical loads.

Fundamental question

What are the effects of characteristic frequencies in the LLJ, if any, on the response of the wind turbine.

The Low Level Jet (LLJ) in the U.S.

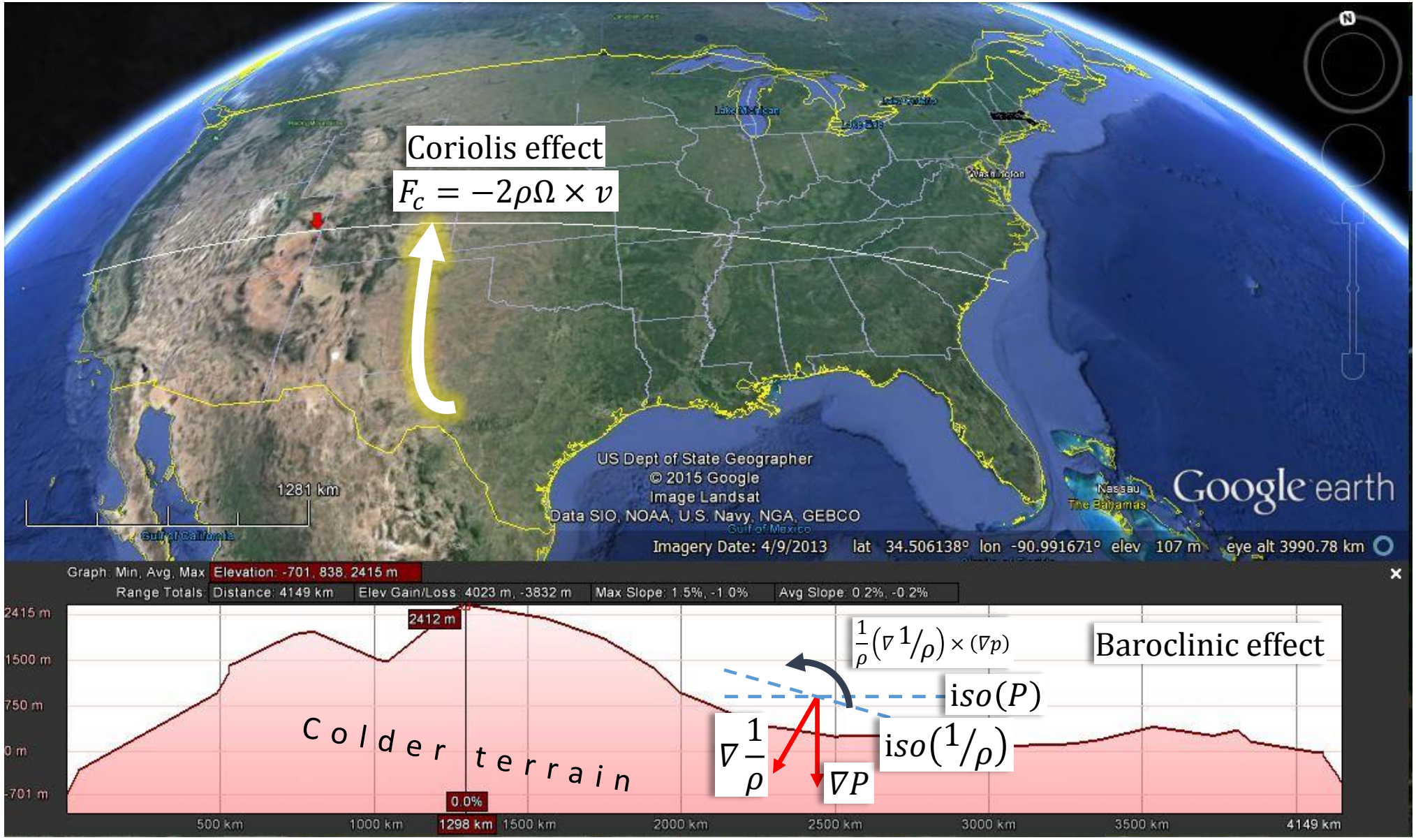

PROBABLE CAUSES:

- Inertial oscillation
- Shallow baroclinicity
- Terrain effects
- Isallobaric forcing
- Vertical parcel displacement

STATISTICS:

- 63 % of nightime. [1]
- Mostly southerly. [1]
- 28 % northerly. [1]
- Peak most frequent at 200-400 m. [1]
- Strongest jets above 300 m. [1]
- Most frequent in the Kansas-Oklahoma border. [2]

[1] Song et al 2005.

[2] Bonner 1968.

Impacts on wind turbines.

TRENDS IN TIP HEIGHT

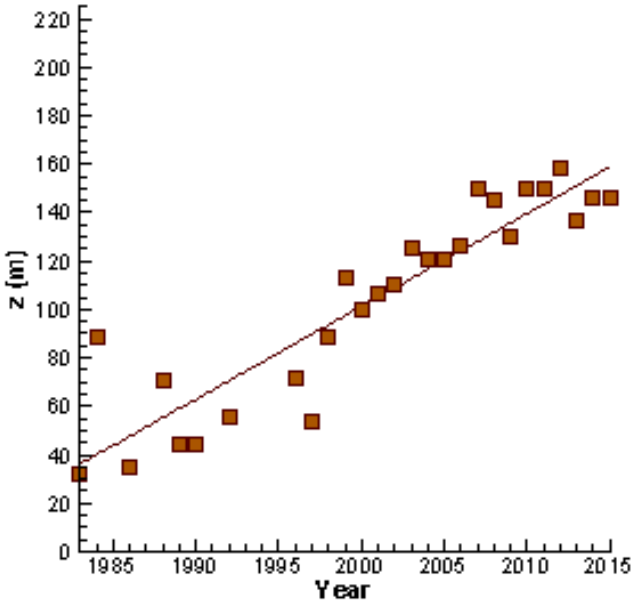

a) Trend in tip heights (USA)

b) World's tallest turbine (Denmark)

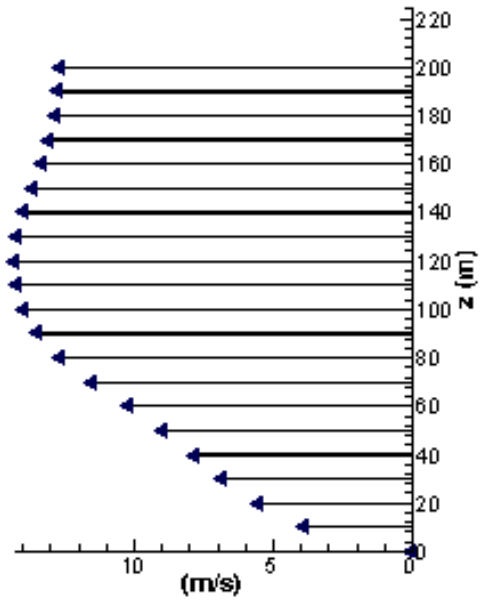

c) LLJ speed profile (USA)

INSTALLED CAPACITY
(US Energy Information Administration)

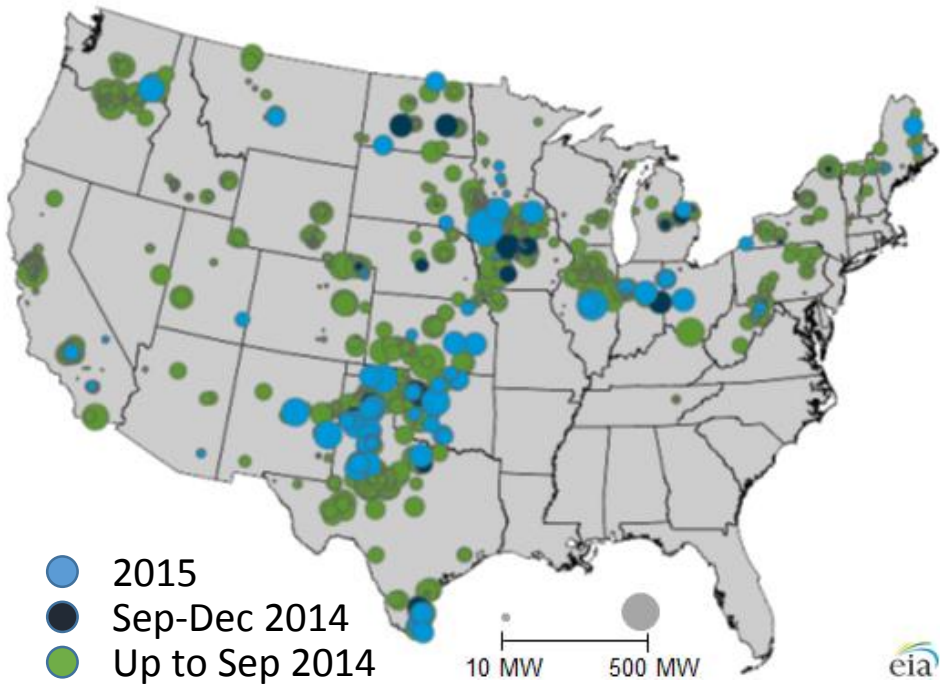

Kelley, 2011:

- found that fatigue loads on the wind turbines were probably associated with the coherent structures derived from a small range of vertical stability usually connected with LLJs and,
- those coherent structures occurred most frequently and were most intense within the stability range of +0:01 < Ri < +0:05, concurring with the range on which the greatest fatigue damage takes place

Experimental data and analysis.

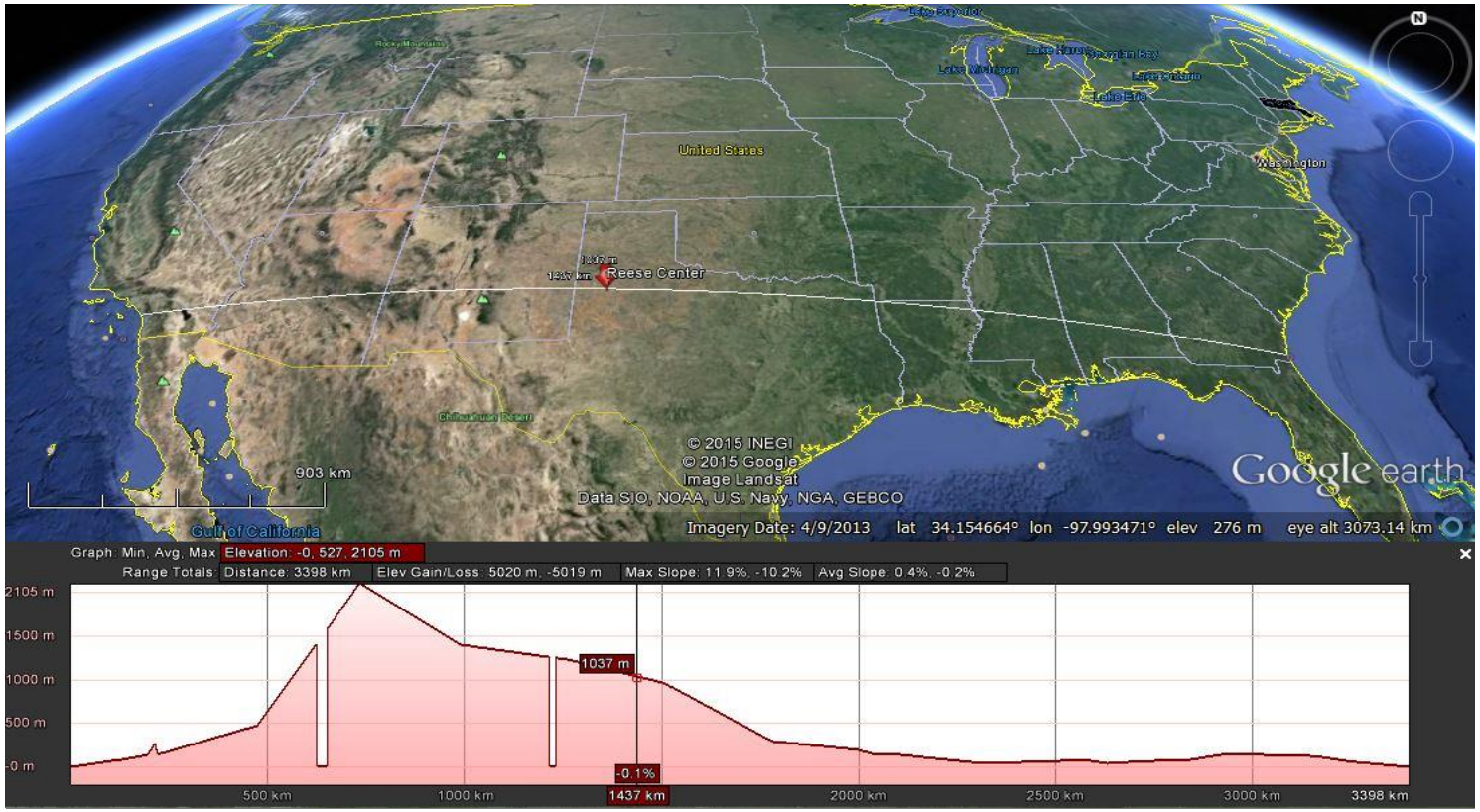

200 m tower

Measurement heights (10 levels):
0.9; 2.5; 4; 10; 17; 47; 75; 116; 158; 200 m AGL

Frequency: 50 Hz (every 0.02 secs.)

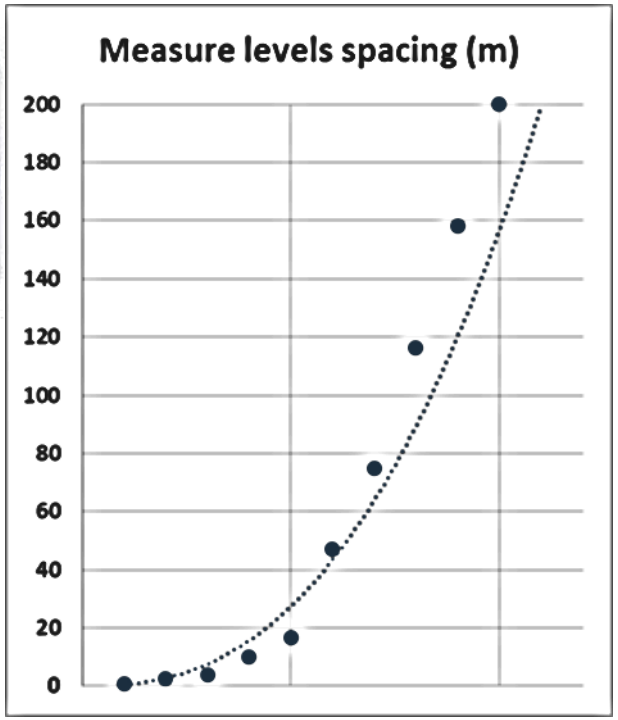

Spacing fit:

$$U = 1.42 \times z^{0.38}$$

Time fills space:

- Interpolation.
- Taylor frozen hypothesis.

MET tower parameters

Location	Reese Center, Lubbock, TX, USA
Altitude	1019 m
Controlled variables	3D wind speed, temperature, pressure, humidity
Frequency	**50 Hz**
Levels	1, 2, 4, 10, 17, 47, 75, 116, 158, 200 m AGL

- 1 year of data was scanned.
- Jets analyzed according to height, speed and profile shape.
- Selection: 22-23 October 2013

Experimental data and analysis.

FAST:

- Fatigue, Aerodynamics, Structures, and Turbulence.
- Comprehensive aeroelastic simulator.
- Predicts both the extreme and fatigue loads
- For 2- and 3-bladed horizontal-axis wind turbines (HAWTs).

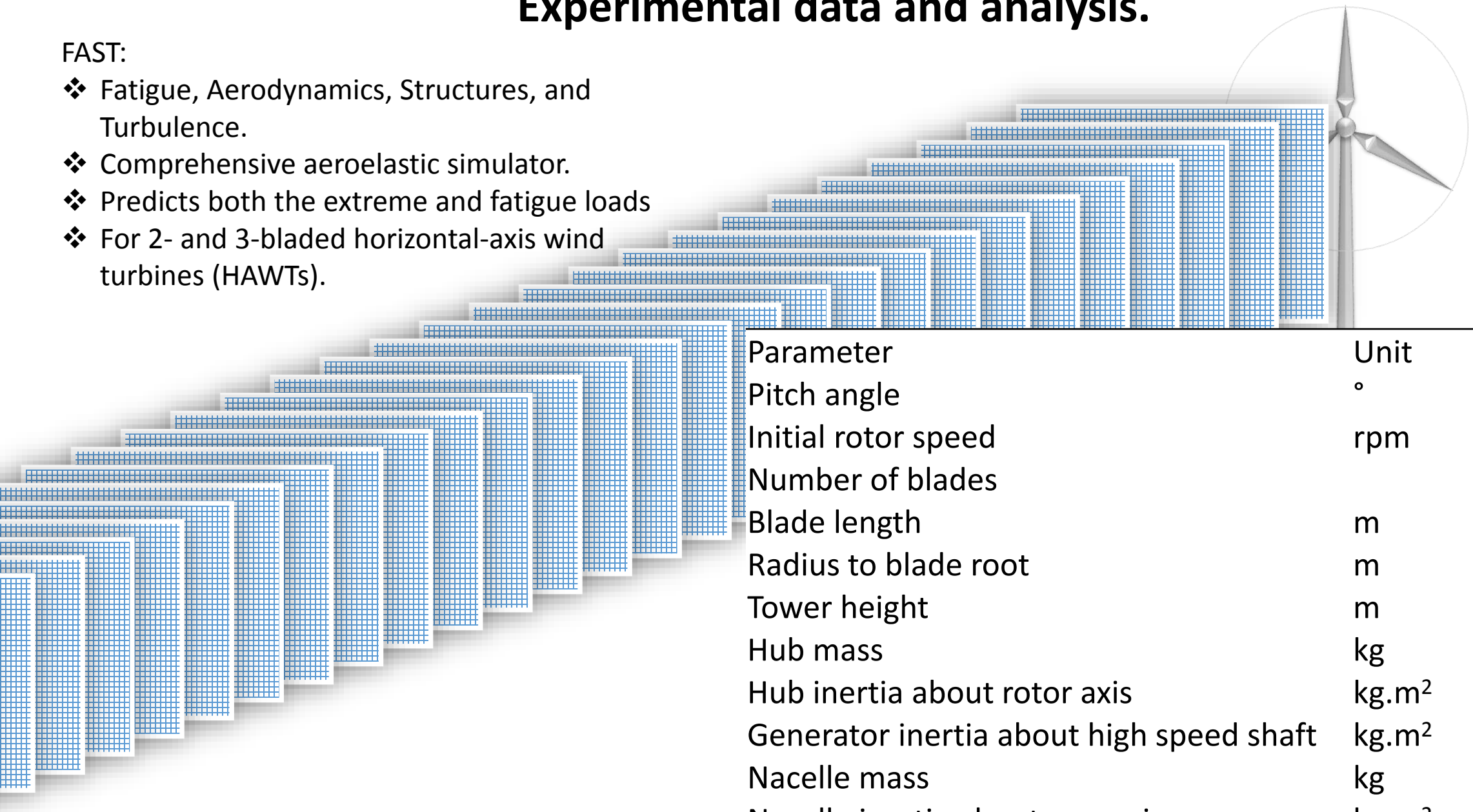

Parameter	Unit	Value
Pitch angle	°	3.5
Initial rotor speed	rpm	32
Number of blades		3
Blade length	m	35
Radius to blade root	m	1.75
Tower height	m	84
Hub mass	kg	15148
Hub inertia about rotor axis	$kg.m^2$	34600
Generator inertia about high speed shaft	$kg.m^2$	53
Nacelle mass	kg	51170
Nacelle inertia about yaw axis	$kg.m^2$	49130

Energy analysis.

Power density ratio:

$$\frac{Pd_{LLJ}}{Pd_{unstable}} = 2.57 \; @ \; z = 120 \; m$$

Wind shear: $ws = \frac{\partial U_{xy}}{\partial z}$

Turbulent kinetic energy:

$$TKE = \frac{1}{2}(\sigma_u^2 + \sigma_v^2 + \sigma_w^2)$$

Richardson number:

$$Ri = \frac{\frac{g}{\theta}\frac{\partial \theta}{\partial z}}{\left(\frac{\partial U_{xy}}{\partial z}\right)^2}$$

Kelley

- Most damaging fatigue loads occur within the weakly stable range of $+0.01 \leq Ri_{grad} < +0.05$, (intense vertical mixing).
- Maximum damage at a value of $Ri_{grad} = +0.02$

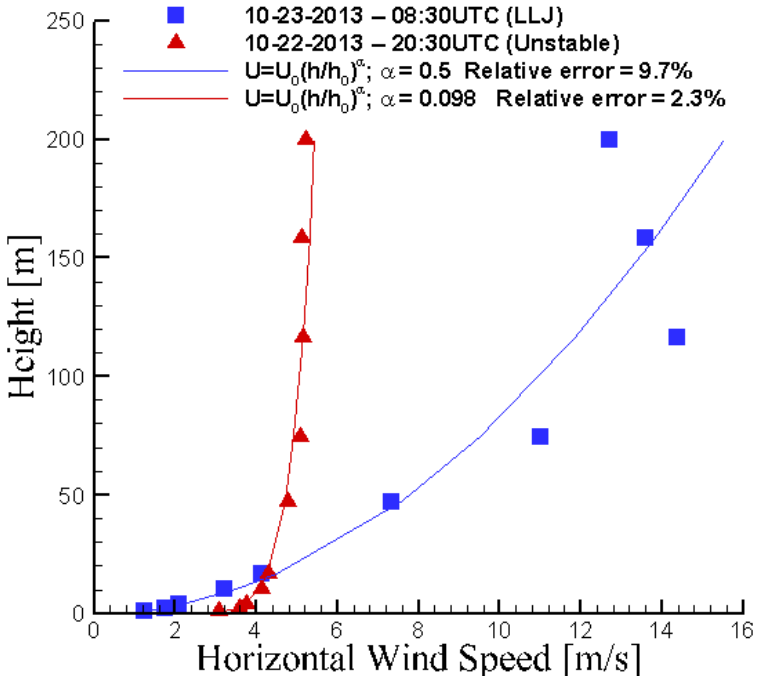

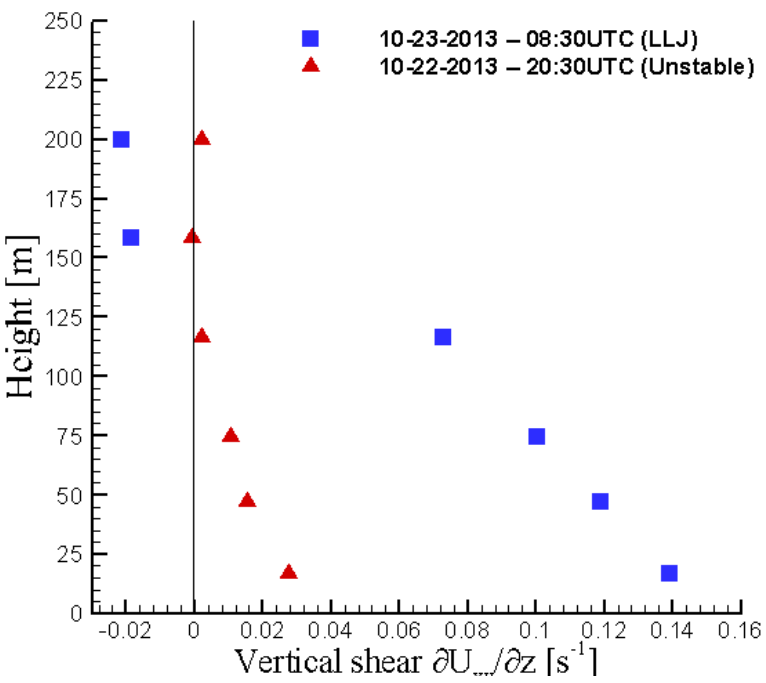

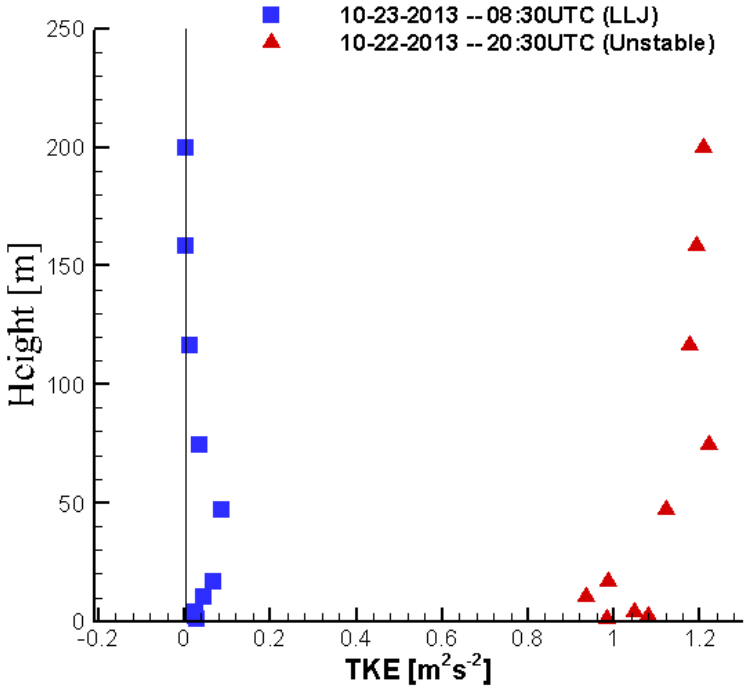

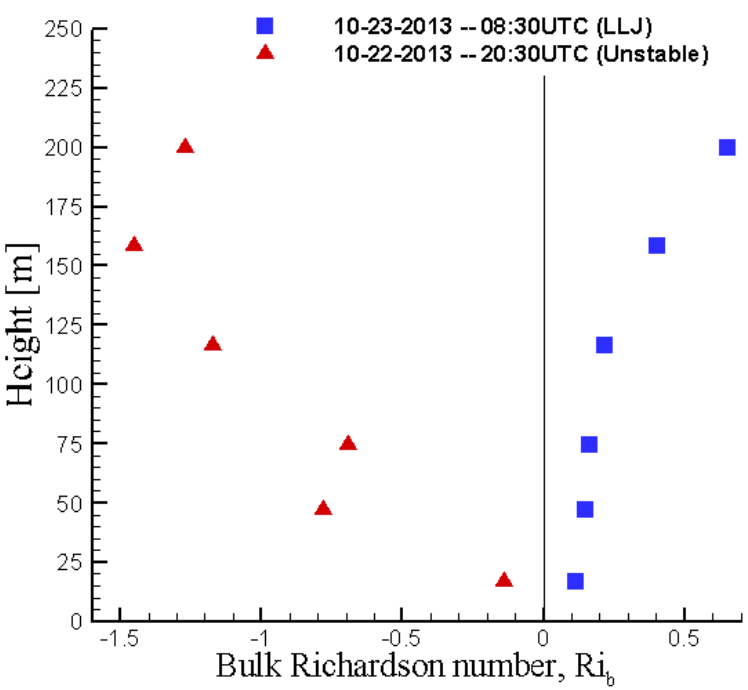

Two point correlations in the vertical direction.

(Reference point: $z_0 = 120\ m$)

$$\rho_{(x,y)} = \frac{E\left[\left(X - \mu_{(x)}\right)\left(Y - \mu_{(y)}\right)\right]}{\sigma_x \sigma_y}$$

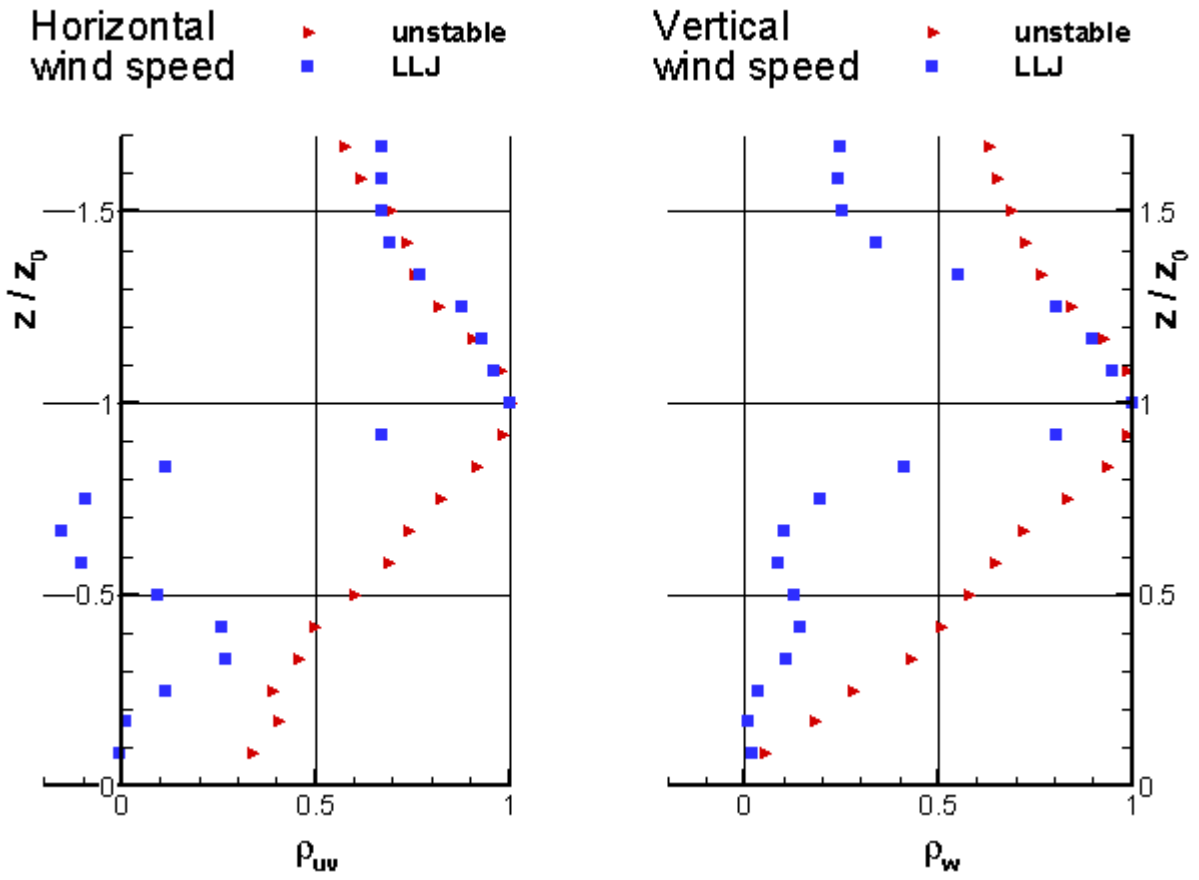

UNSTABLE CONDITIONS:

- Good correlation in $0.3 \leq \frac{z}{z_0} \leq (more\ than\ 1.7)$.
- Correlation in $0 \leq \frac{z}{z_0} \leq (more\ than\ 1.7)$.
- Decrease linearly upward and downward.
- Evidence of convective mixing.
- Layer interactions: Buoyancy + viscous.

LLJ:

- Good correlation in $0.9 \leq \frac{z}{z_0} \leq (more\ than\ 1.7)$ for U_{xy}.
- Good correlation in $0.9 \leq \frac{z}{z_0} \leq 1.4$ for U_z.
- Correlation in $0.7 \leq \frac{z}{z_0} \leq (more\ than\ 1.7)$.
- Deteriorates abruptly below the nose for both velocities.
- Deteriorates abruptly upward for vertical velocity.
- Evidence of layer independence.
- Layer interaction: viscous.

Vertical thickness of the LLJ:

$$\frac{z}{z_0} \approx 0.7 \quad \Longrightarrow \quad \Delta z \approx 35\ m\ below\ the\ peak$$

LLJ influence: $40 \leq z \leq 260\ m$

Autocorrelations and integral length scale in the horizontal direction.

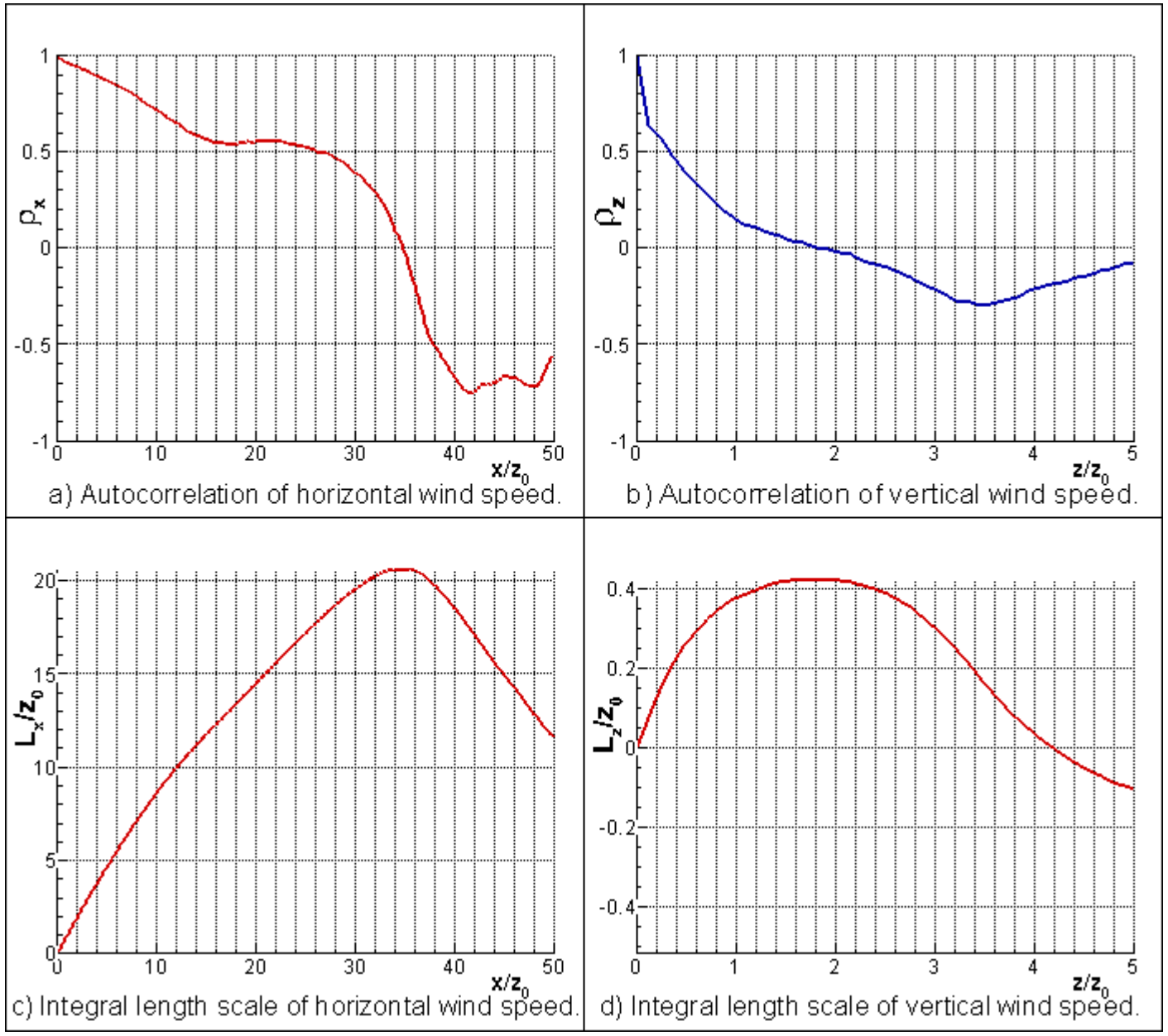

$$\rho_{(x,y)} = \frac{E\left[\left(X - \mu_{(x)}\right)\left(Y - \mu_{(y)}\right)\right]}{\sigma_x \sigma_y}$$

$$L = \bar{U} \int_0^{\infty} \rho_{(t)} dt$$

Taylor frozen hypothesis converts time into space.

Horizontal velocity is correlated: $\frac{x}{z_0} \leq 32$

Vertical velocity is correlated: $\frac{x}{z_0} \leq 1.8$

Effects of de-trending

- **Instantaneous**: autocorrelation and ILS with instantaneous values.
- **De-trend**: intervals of 40 s, a mean velocity per interval. Prime is calculated as instantaneous minus mean and correlation is calculated with prime.
- **Moving average**: similar to previous but mean is calculated as average 20 s before and after the instantaneous point. It avoids the discontinuity effect.

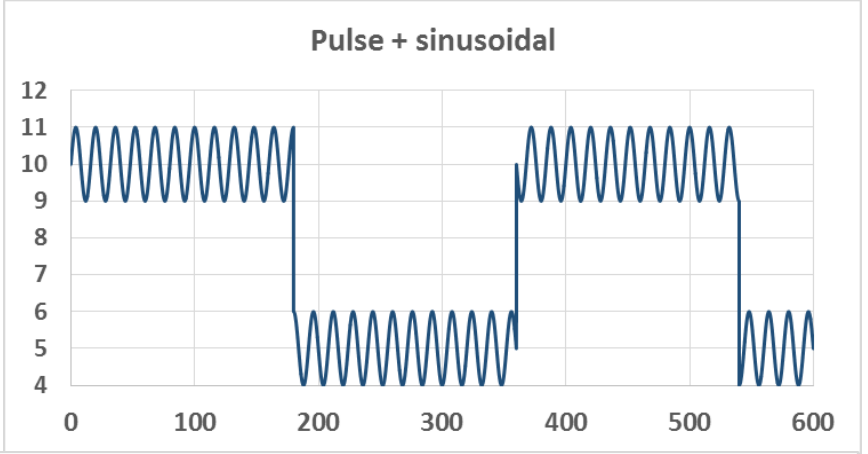

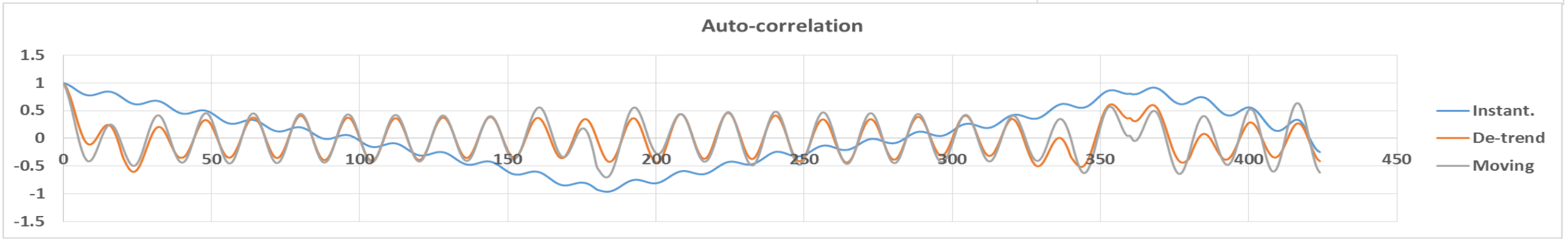

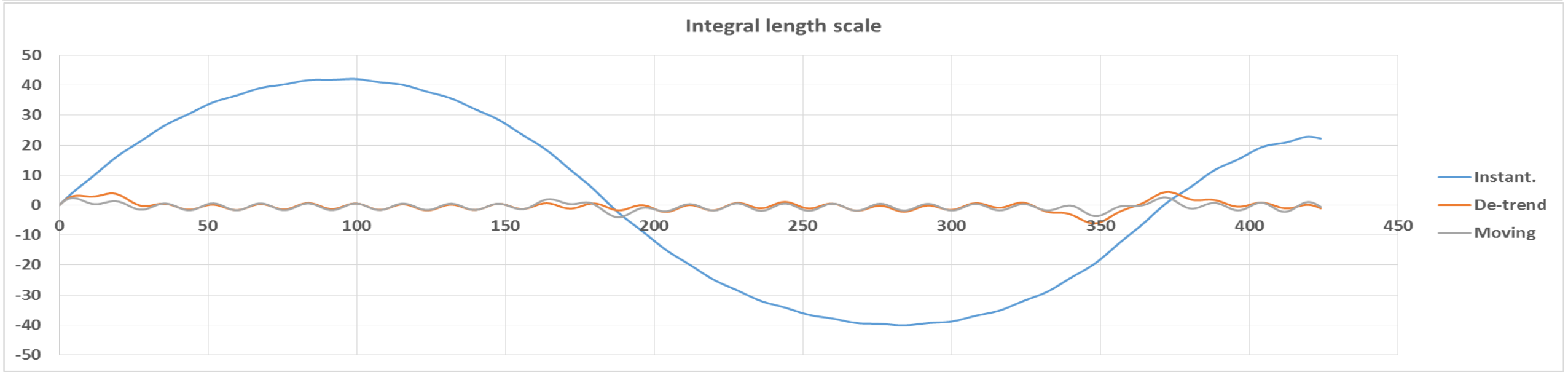

Autocorrelations and integral length scale in the horizontal direction.

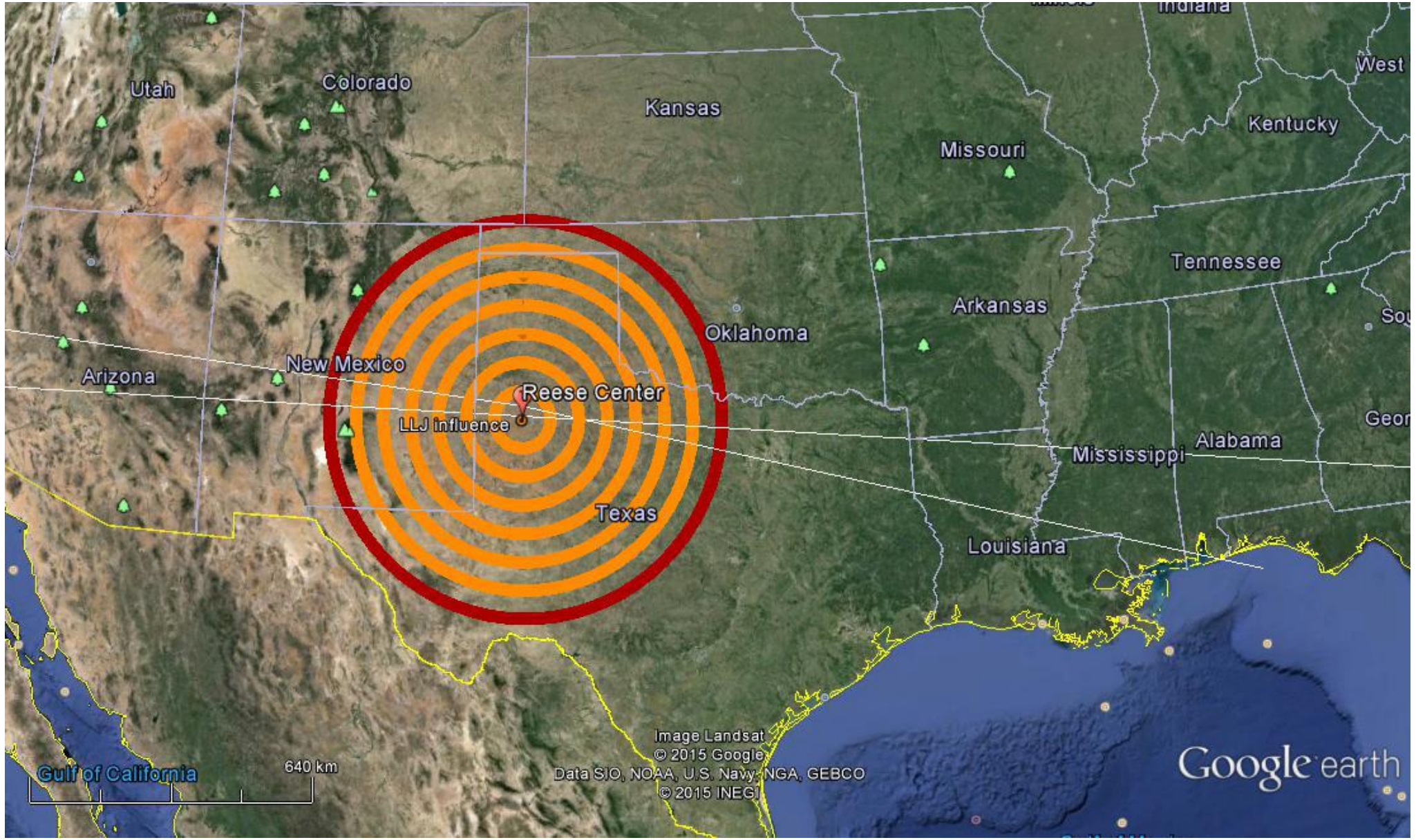

Correlation at peak of maximum strength:

$x \approx 54\ km$

Taylor frozen hypothesis for the whole incident:

$x \approx 400\ km$

Correlation of fluctuations:

$x \approx 200\ m$

Autocorrelation of the LLJ horizontal velocity at different levels.

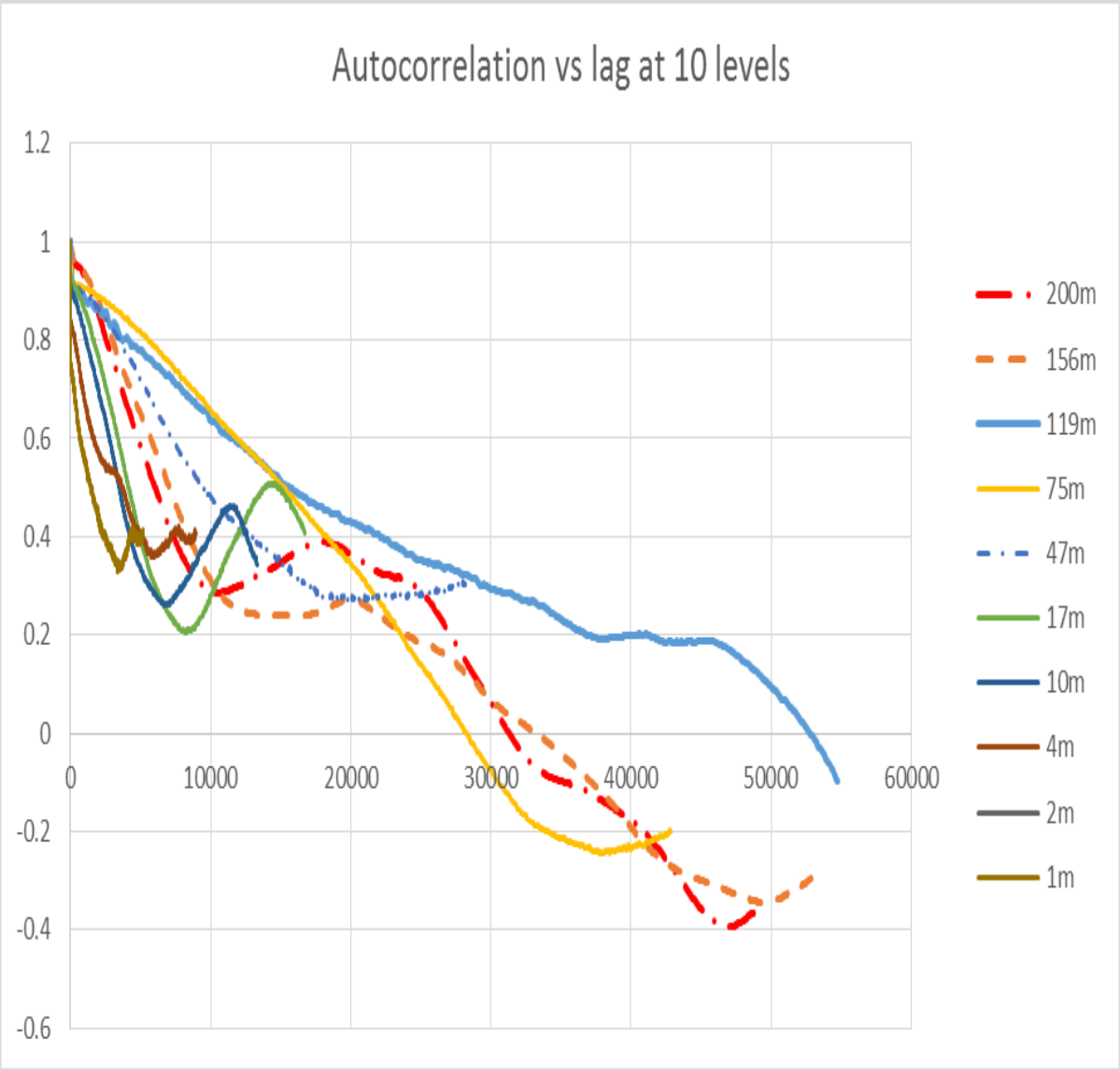

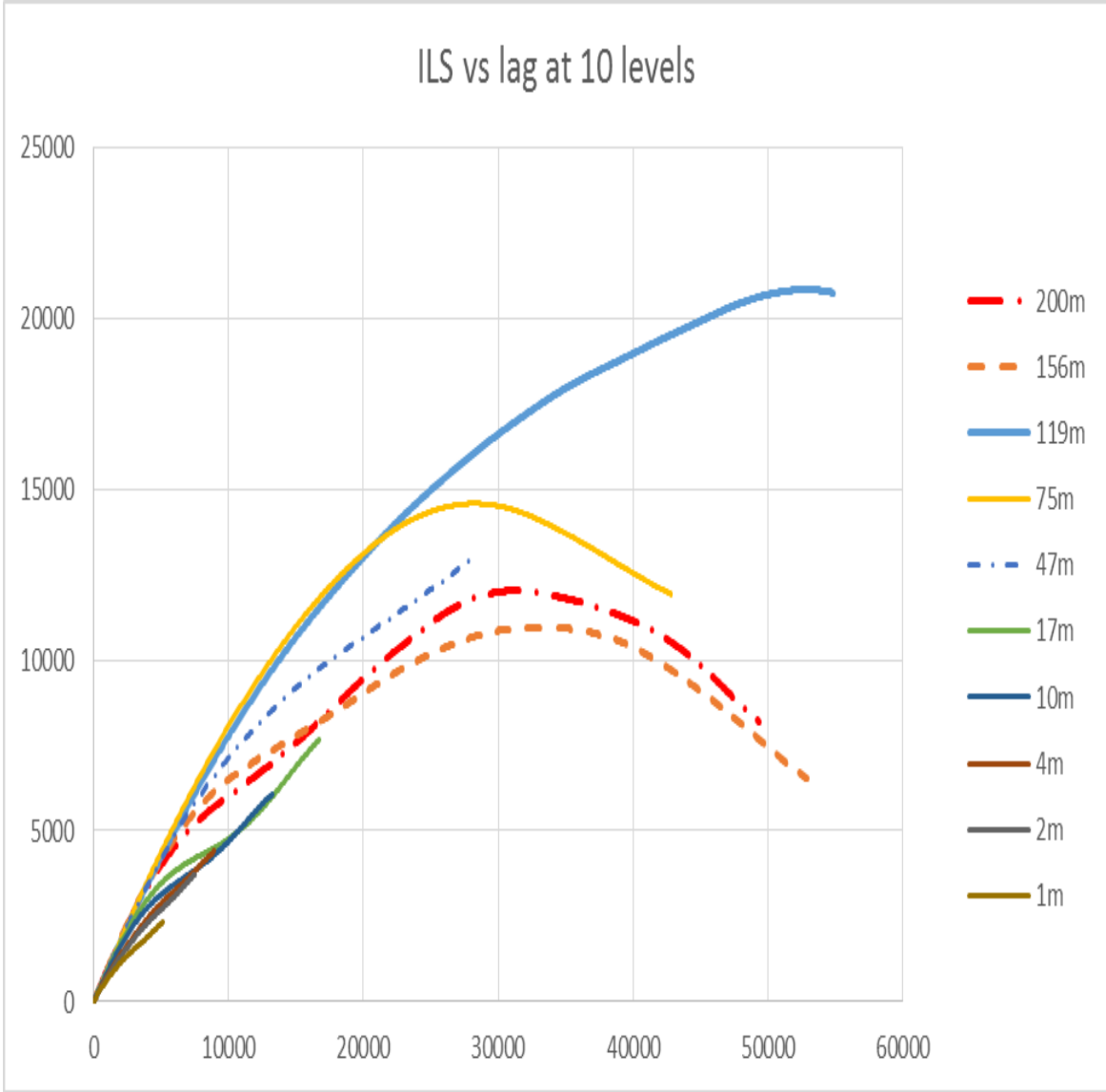

Horizontal length of the LLJ: $x \approx 54000\ m$

Power Spectra Density (PSD) in unstable conditions.

$$PSD_{(\omega)} = \lim_{T\to\infty} E\left(\left|\hat{x}_{T(\omega)}\right|^2\right)$$

$$E_k \approx k^{-5/3}$$

Horizontal velocity

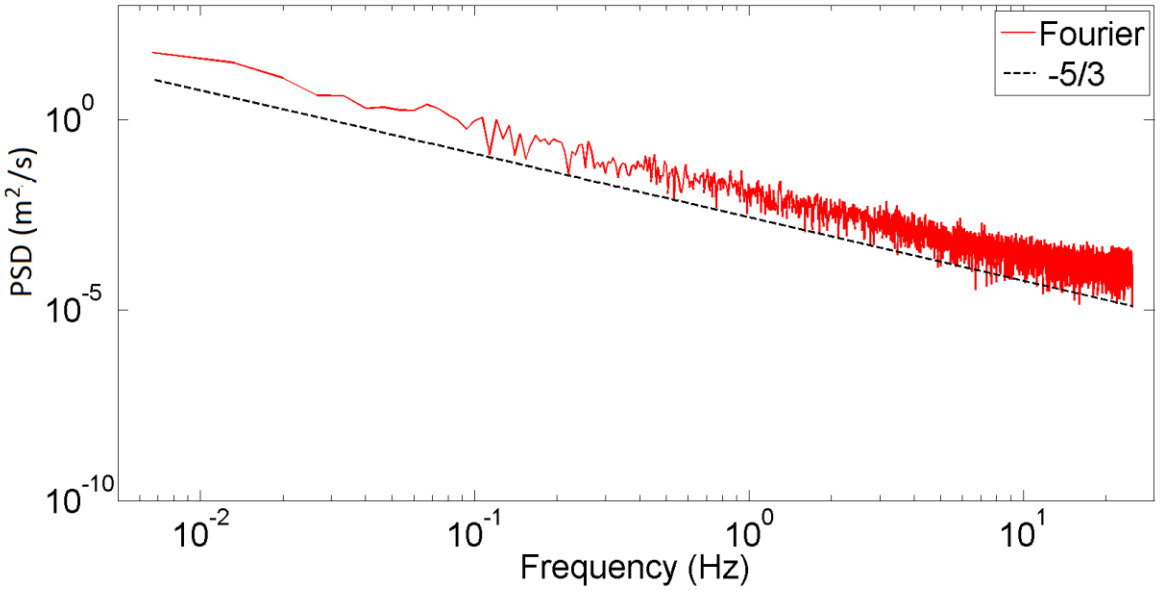

Vertical velocity

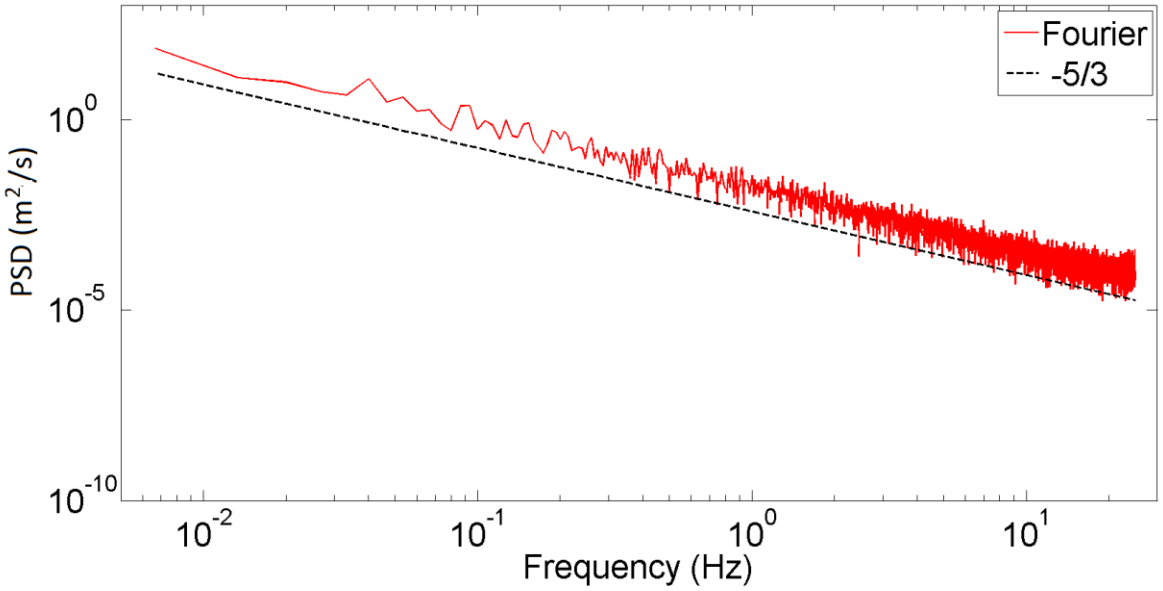

158 m

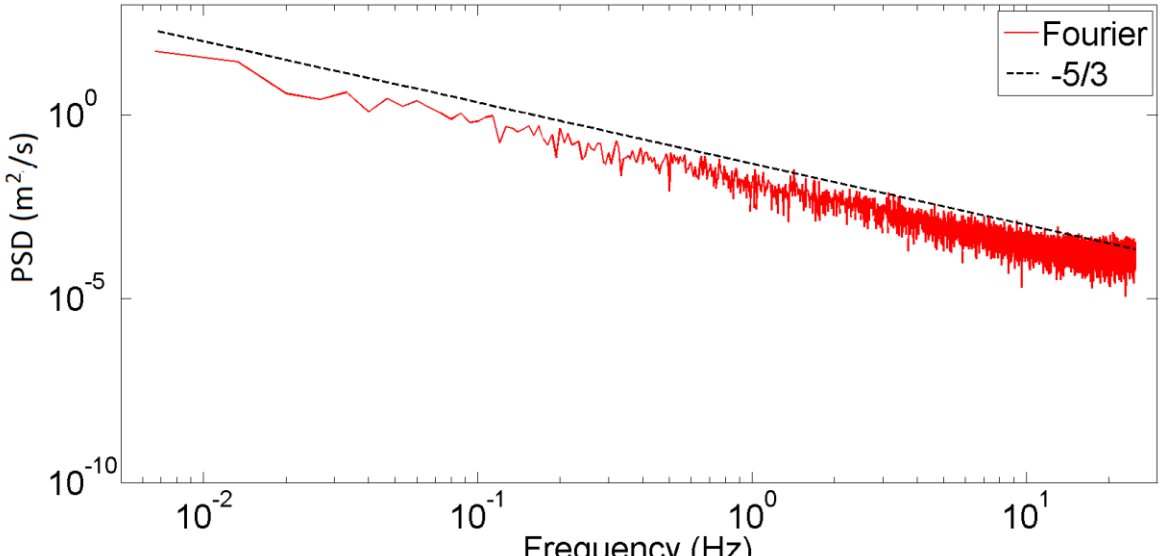

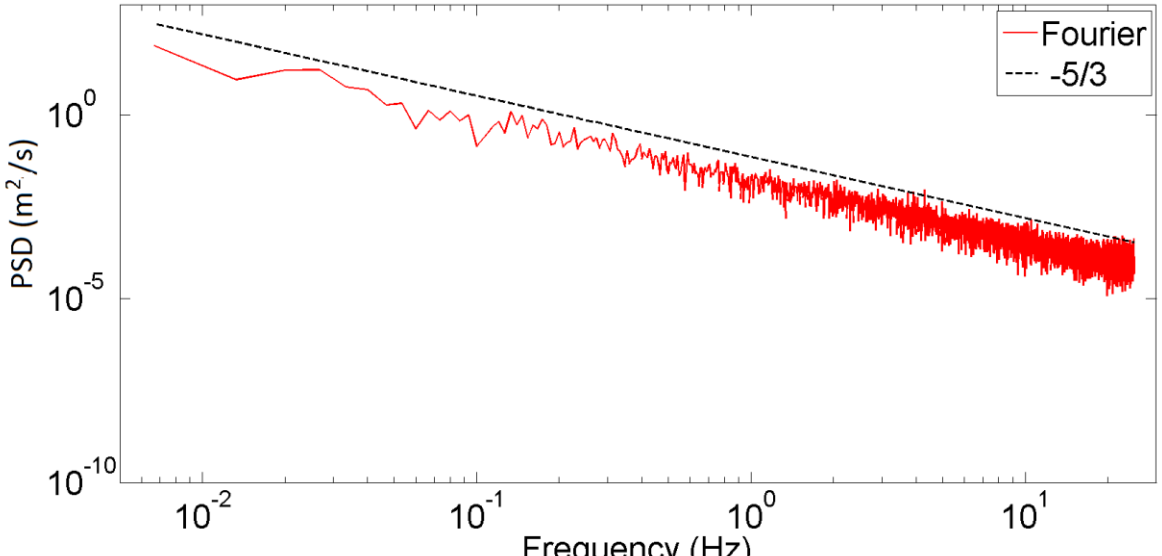

116 m

Power Spectra Density (PSD) in LLJ.

$$PSD_{(\omega)} = \lim_{T\to\infty} E\left(\left|\hat{x}_{T(\omega)}\right|^2\right)$$

Horizontal velocity

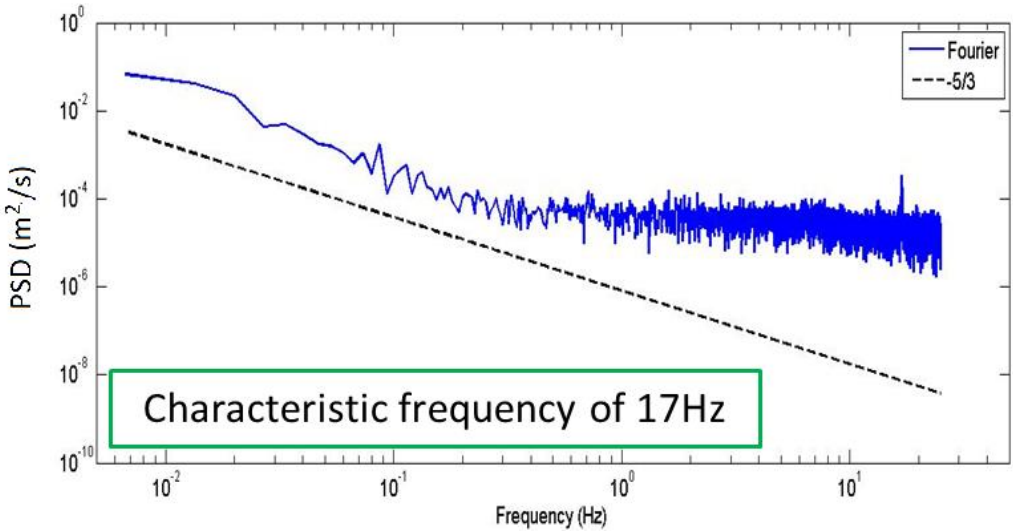

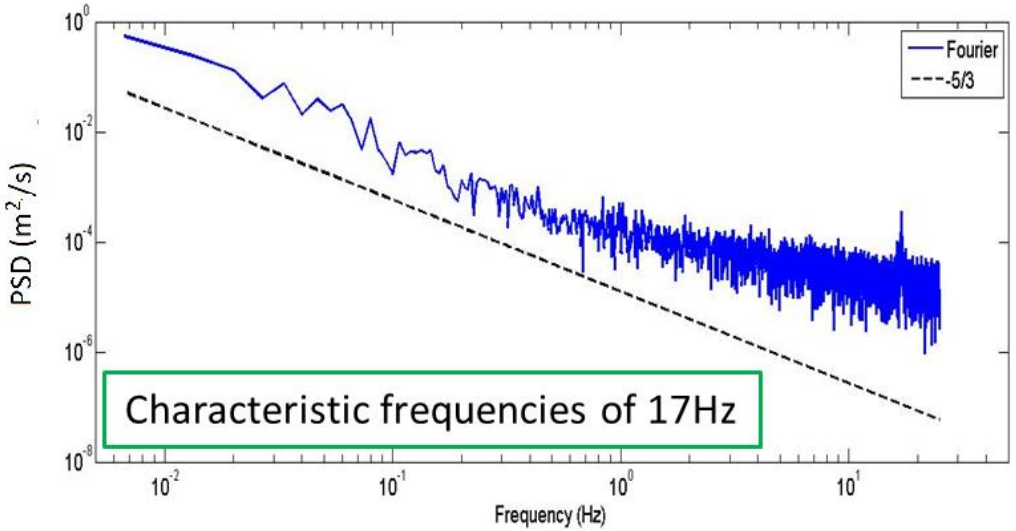

Vertical velocity

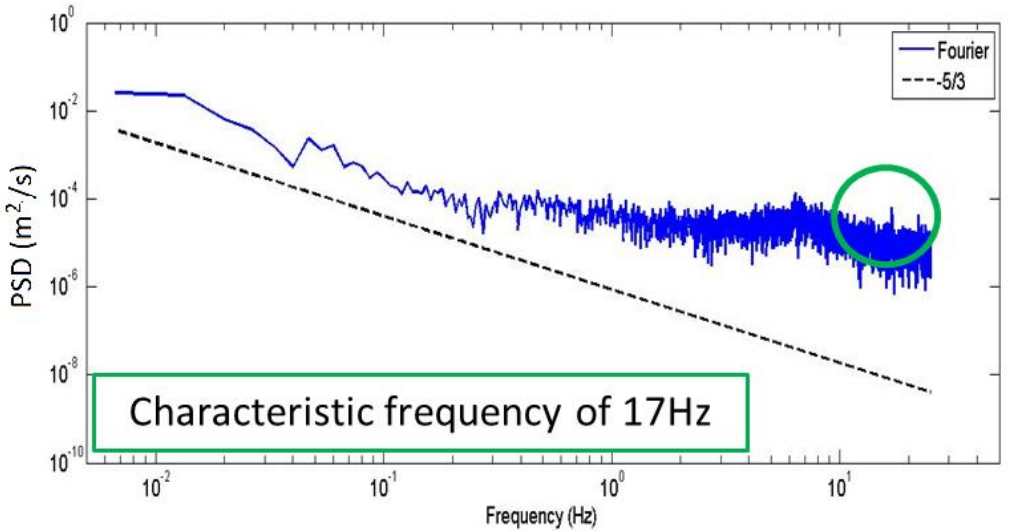

158 m

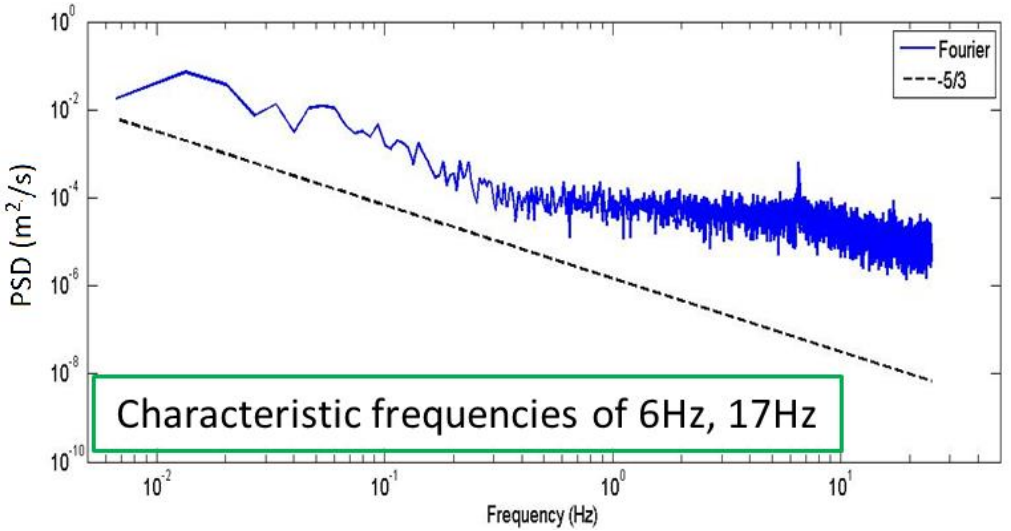

116 m

- Anisotropy.
- Exacerbation of specific modes.

Wind turbine responses

IN-PLANE TIP DEFLECTION [m]

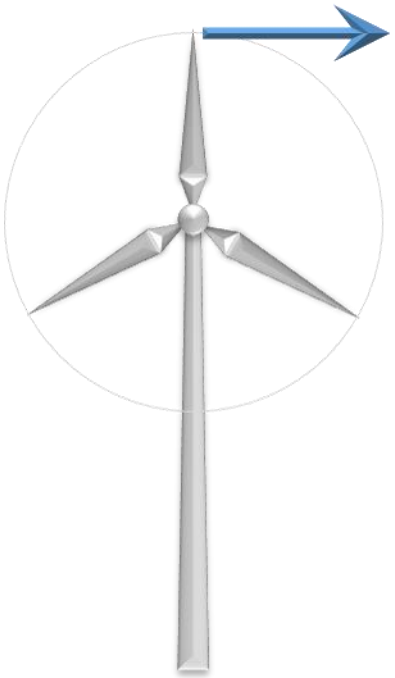

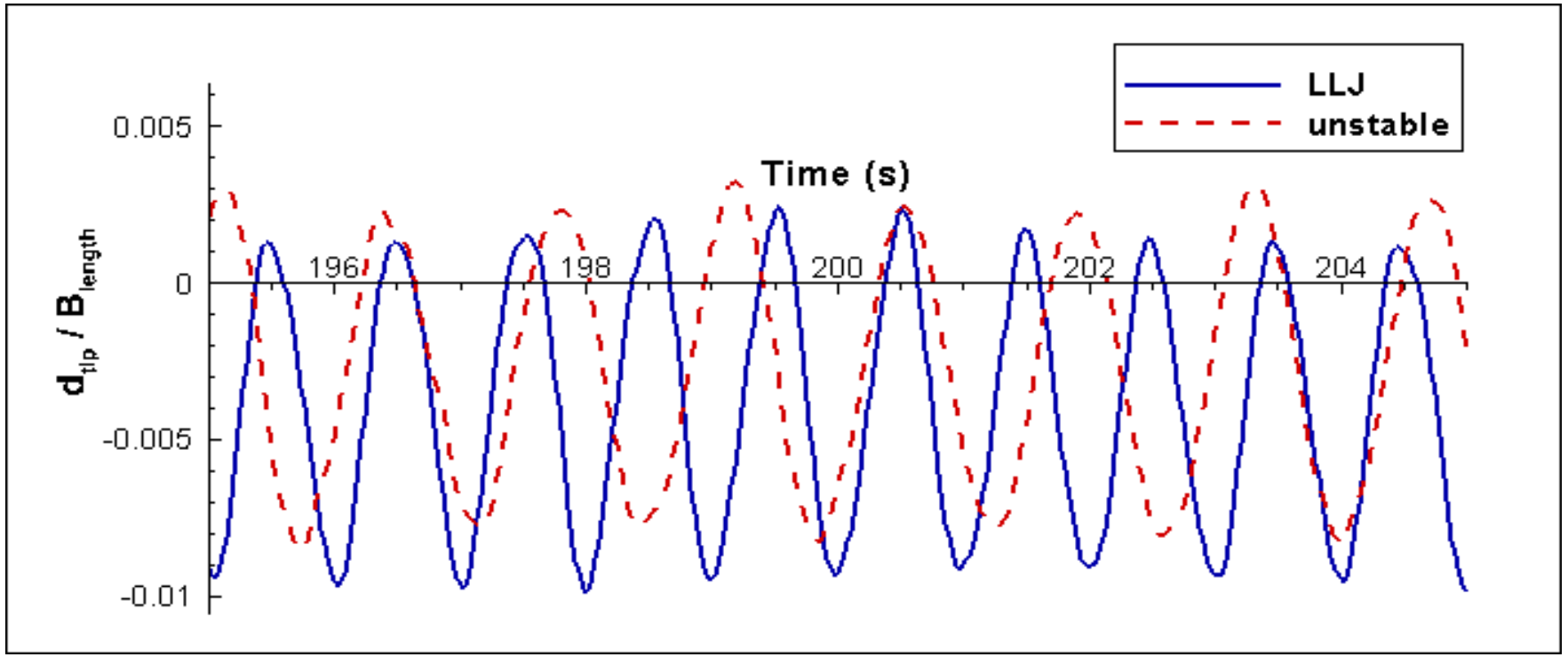

$\bar{d}_{LLJ} = -0.131$ m $\quad \sigma_{LLJ} = 0.138$ m

$\bar{d}_{noLLJ} = -0.099$ m $\quad \sigma_{noLLJ} = 0.132$ m

	unstable		LLJ	
	rpm	Hz	rpm	Hz
Min	21.61	0.36	55.41	0.92
Max	32.36	0.54	77.93	1.30
Mean	27.56	0.46	65.95	1.10
Range	27.81	**0.46**	66.30	**1.10**

Wind turbine responses.

FLAPWISE MOMENT (CAUSED BY FLAPWISE FORCES) AT THE BLADE ROOT [kN.m]

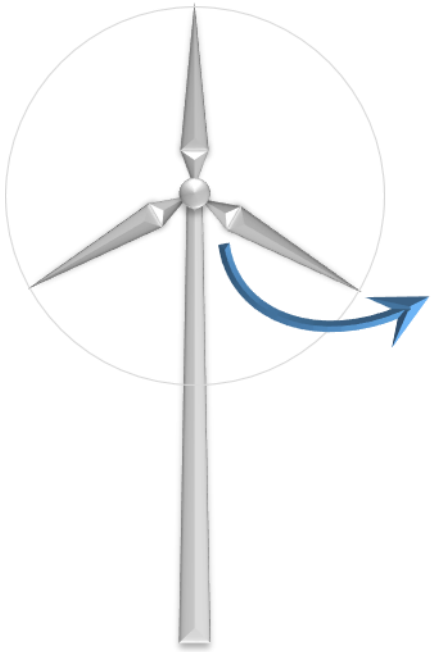

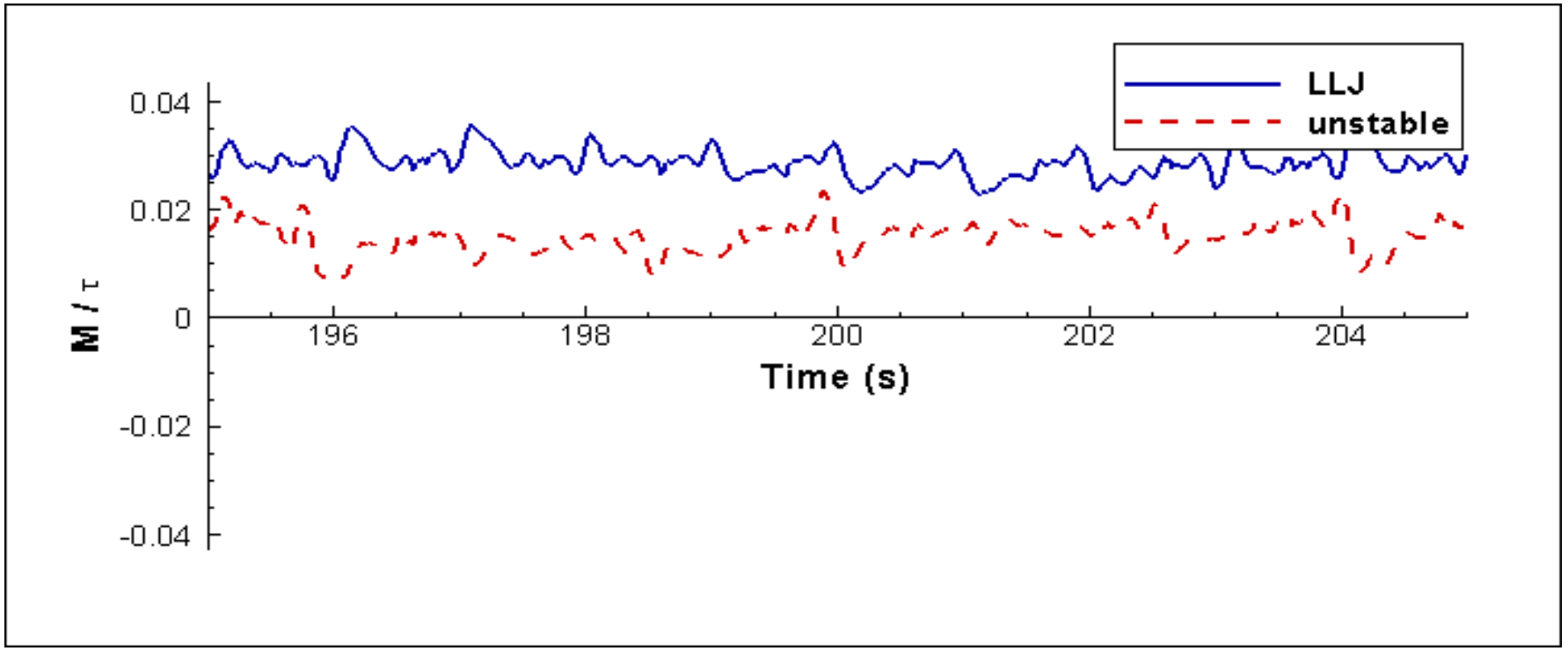

$\bar{M}_{LLJ} = 933\ kN.m$ $\sigma_{LLJ} = 261\ kN.m$

$\bar{M}_{noLLJ} = 593\ kN.m$ $\sigma_{noLLJ} = 178\ kN.m$

	Momentum (kN.m)		Tip deflection (m)		Frequencies
	Mean	Deviation	Mean	Deviation	(Hz)
LLJ	933	260	-0.131	0.138	1.1; 6; 17
unstable	593	178	-0.099	0.132	0.7

- LLJ imposes larger static and dynamic loads and more fatigue cycles over the structure.
- For oscillations with higher amplitude, LLJ oscillates at more than twice the frequency (1.1 Hz vs 0.5 Hz).

Power spectra of in-plane blade tip deflection.

LLJ

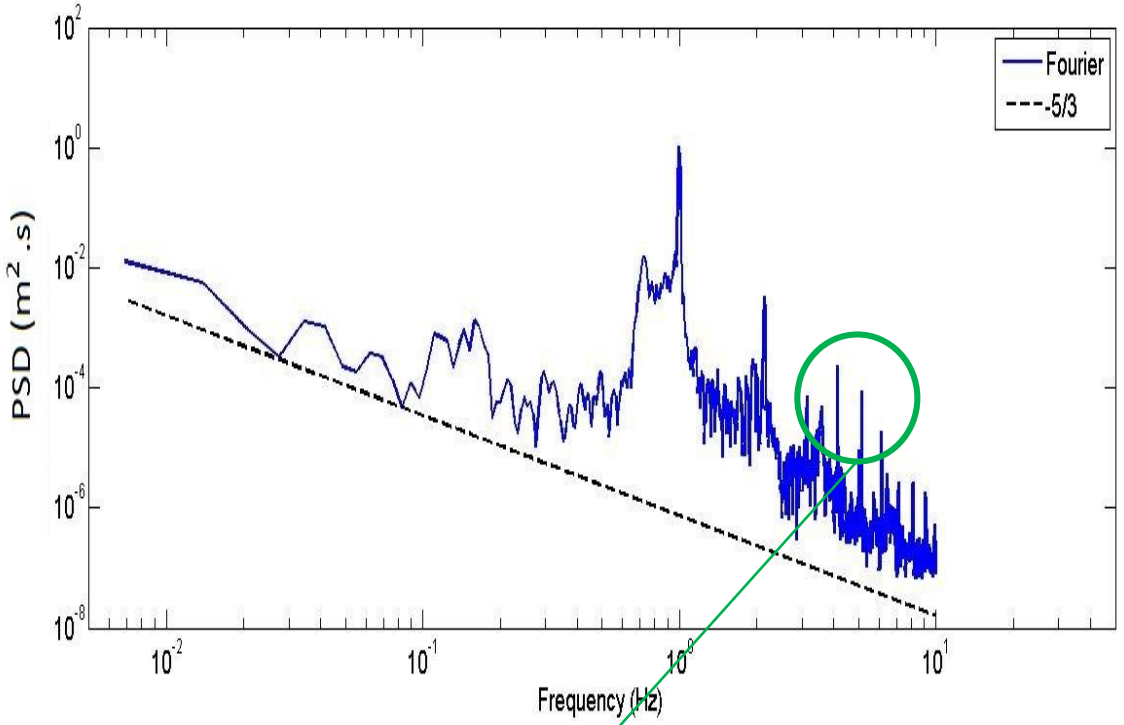

These characteristic frequencies are close to one of the natural frequencies of vertical velocity ~ 6Hz

Unstable

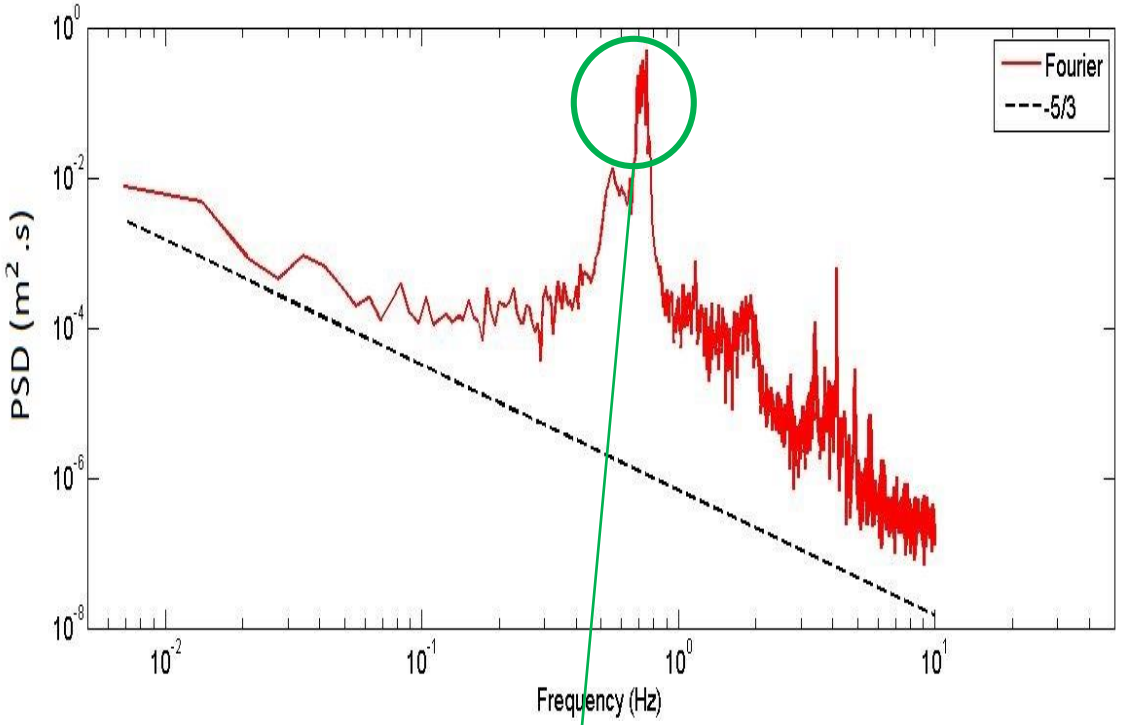

This mode oscillates at a lower characteristic frequency (0.7Hz) than that of the LLJ case (1Hz)

Power spectra of flapwise bending moment.

LLJ

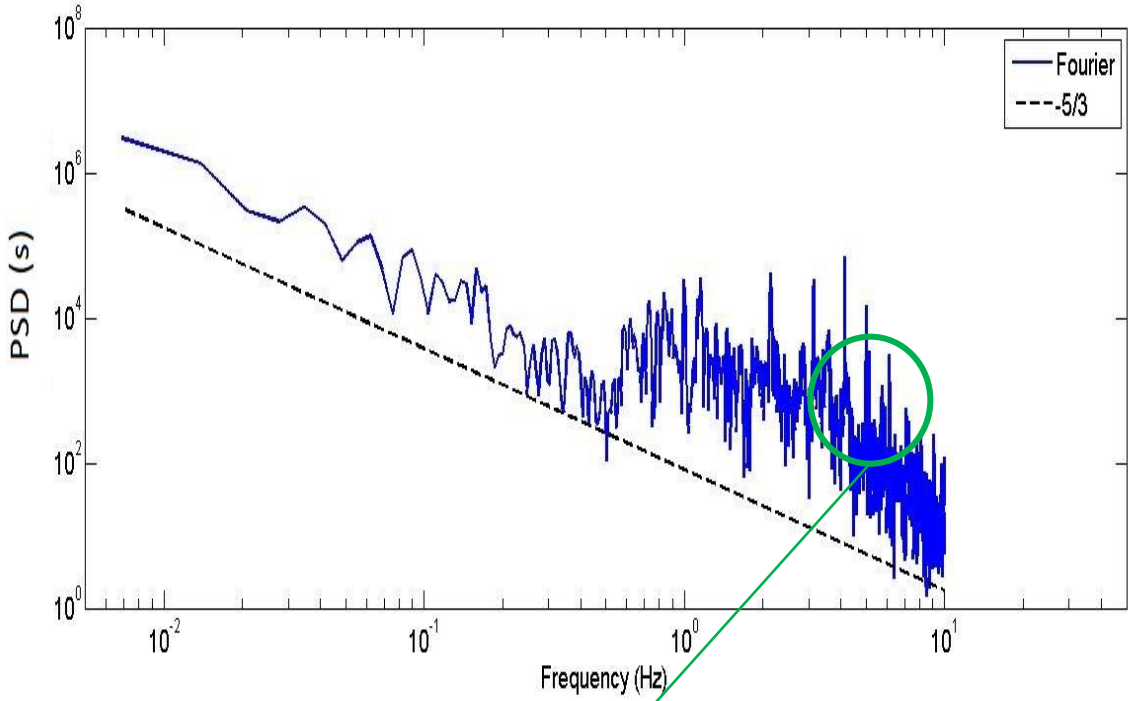

These characteristic frequencies are close to one of the natural frequencies of vertical velocity ~ 6Hz

Unstable

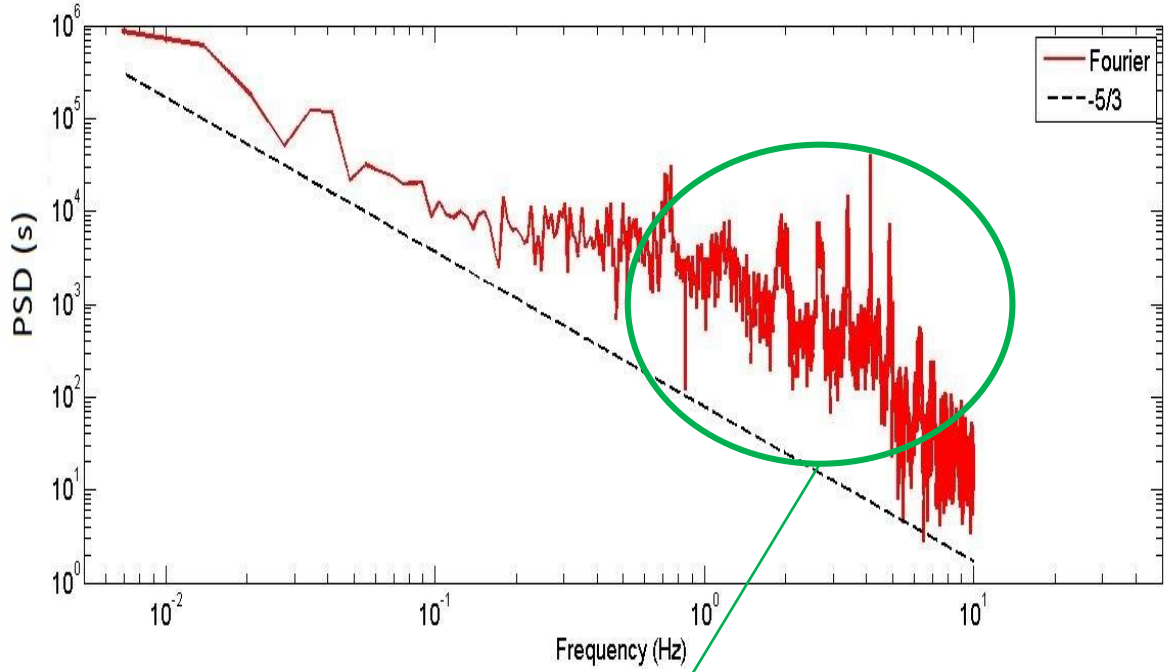

Less “noisy” oscillations than those with LLJ

- Across-the-plane motion is restricted down to the foundation.
- Action-reaction moments stimulate the formation of bending oscillations.

Conclusions (1/2)

- We have determined the characteristics length scales and other parameters of a LLJ.
- Vertical thickness was approximately $\frac{z}{z_0} \approx 0.7$ which corresponds to approximately 35 m below the nose.
- Based on the jet vertical dimensions and size of tallest turbine, the region of interest for interactions wind turbines – LLJ goes from 40 to 260 m.
- The smaller wind turbines with upper tip height <40 m receive negligible impact from LLJs.
- Most current utility-scale wind turbines and the future wind turbines are affected by LLJs.
- Turbulent kinetic energy (TKE) and turbulent intensity are significantly lower for the LLJ but the energy concentrates in particular frequencies of oscillations that stress the turbine.
- The application of the inertial sub-range in the Kolmogorov scale is valid in unstable conditions, indicating a fast dissipation of energy. Isotropy is favored by the convective mixing.
- In LLJ, assumption of isotropy is weakened by the existence of directional alignment derived from a long coherence of the LLJ structure. A slower rate of energy transfer is obtained when vortices degrades into smaller vortices.
- Characteristic frequencies of approximately 6 Hz and 17 Hz were detected in the LLJ below and near the peak and above the peak of the jet.

Conclusions (2/2)

- Due the increase in wind velocity, the LLJ augmented the wind power density more than 2.5 times at the heights of the rotor area, which means it can deliver substantially more electric power.
- LLJ impose a variety of mechanical loads over the wind turbine, including increases of static and mechanical loads and also fatigue cycles due primarily to sustained high energy and the high wind shear.
- The in-plane tip blade deflection oscillated 37 % faster and mean deflection increased 67 %.
- The flapwise moment oscillated at more than twice the frequency compared with unstable conditions.
- The match of characteristics frequencies between the incoming wind and the turbine signals demonstrates that the turbine can mimic the signals from the incoming wind.
- Wind signal replication can be attenuated, shifted or annulled by the turbine as the output signals results from a combination of incoming wind and the characteristics of the turbine.
- Characteristic frequencies of the turbine due to rotation (0.7 to 1Hz) provoke peaks in PSD of blade tips.
- Turbine responses across the plane of rotation differs from responses in the plane of rotation. While there is a degree of freedom in the direction of the turbine rotor rotation, motion is restricted axially, stimulating the formation of bending oscillations.

Structural Impact Assessment of Low Level Jets over Wind Turbines

END OF PRESENTATION

Grant: NSF-CBET #1157246, NSF-OISE-1243482 and NSF-CMMI #1100948

Presentation
for NAWEA Symposium 2015,
Blacksburg, VA.